Sub-Optimum Detection of Coded Continuous Phase Modulation in Radio Channels

Francisco A. Monteiro, António J. Rodrigues
Instituto de Telecomunicações / Instituto Superior Técnico, Technical University of Lisbon
Av. Rovisco Pais, 1049-001 Lisbon, Portugal
Tel: +351 218418487; Fax: +351 218418472; E-mail: frmo@lx.it.pt

Abstract

This paper presents a practical receiver for coded continuous phase modulation (CPM) intended for wireless communications in TDMA/FDMA modes. The coded CPM is interpreted as a single Markov chain. Usage of simultaneous complexity reduction techniques is proposed. Only two correlators (I and Q) are used as a front-end, both operating on over-sampling mode and projecting the received signal into a space of Walsh functions. Those metrics are fed to a reduced states sequence detector (RSSD) using the search algorithm, which is a generalised Viterbi decoding. A strong reduction in memory requirements is accomplished. The implications are studied for a known optimum concatenation: (8-ary; h=1/6) CPM with a rate 2/3 convolutional encoding.

Key Words: CPM; convolutional encoding; Walsh space projections; search algorithm.

I. INTRODUCTION

Continuous phase modulation has now an history of 20 years [1,2]. Although continuous phase modulation (CPM) has rather good characteristics for wireless communications, its application is still restricted to some expensive fixed wireless access (FWA) equipments. By using CPM one gets a modulated signal with constant amplitude and its phase continuity permits a good spectral performance. The imposed phase continuity implies a memory existence that carries out a coding effect revealed in a code gain. Being the information transmitted in the phase evolution, no information is lost if a non-linear amplification is made. Since early times, what is restraining widespread use of CPM is the complex detection process it requires. Actual research in this field is mainly concerned with complexity reduction and the synchronization issue. This paper presents a receiver employing, at the same time, two detection techniques recently proposed for complexity reduction: Walsh functions mapping by over-sampling correlators [3] and the search algorithm [4,5].

A. CPM formatting

A CPM signal is obtained by:

$$s(t,\boldsymbol{\gamma}) = \sqrt{\frac{2E_s}{T_s}}\cos(\omega_c t + \varphi(t,\boldsymbol{\gamma}) + \varphi_0) \tag{1}$$

The carrier frequency, f_c, is hidden in $\omega_c=2\pi f_c$, φ_0 is the arbitrary initial phase and E_s is the energy per symbol. The information is carried by the signal's phase in a way that

$$\varphi(t,\boldsymbol{\gamma}) = 2\pi h\sum_{i=-\infty}^{\infty}\gamma_i q(t-iT_s) \tag{2}$$

The channel symbols are $\gamma_i \in \{\pm1,\pm3,...,\pm M-1\}$ and they form the sequence $\boldsymbol{\gamma}$. A constant modulation index, $h=p/q$, is considered with p and q being integers having no common factors. The phase transition pulse shape, $q(t)$, affects phase transitions during L symbols (L>1 for partial response signalling). $q(t)$ is defined by means of the frequency pulse shape, $g(t)$:

$$q(t) = \int_{-\infty}^{t} g(\tau)d\tau \tag{3}$$

The usual normalisation $q(t) = \int_0^{\infty} g(\tau)d\tau = 1/2$ is applied so that the maximum phase transition during a symbol time, T_s, is $h\cdot(M\text{-}1)\cdot\pi$. Within T_s, φ_i evolves $h\cdot\gamma_i\cdot\pi$. At the end of every interval the phase should lie in one of the following cases:

$$\varphi_i \in \left\{0, \pi\frac{p}{q}, 2\pi\frac{p}{q}, \cdots, (q-1)\pi\frac{p}{q}\right\} \text{ , for } p \text{ even} \tag{4a}$$

$$\varphi_i \in \left\{0, \pi\frac{p}{q}, 2\pi\frac{p}{q}, \cdots, (2q-1)\pi\frac{p}{q}\right\} \text{ , for } p \text{ odd} \tag{4b}$$

Distinct CPM families are defined by the frequency pulse shaping. The most common frequency pulse shapes are: LREC, LRC and GMSK, expressed in (5)-(8).

- LREC (rectangular); when L=1 (Fig. 1) it is also known as continuous phase frequency shift modulation (CPFSK).

$$g(t) = \frac{1}{2}rect\left(\frac{t-LT_s}{LT_s}\right) = \begin{cases}\dfrac{1}{2LT_s}, & 0 \le t \le LT_s \\ 0, & \text{elsewhere}\end{cases} \tag{5}$$

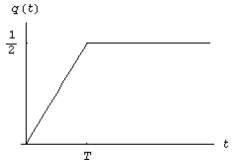

Fig. 1: 1REC pulse phase transition.

From (1) and (2), CPFSK signals can be expressed as

$$s(t) = \sqrt{\frac{2E_s}{T_s}}\cos\left\{2\pi\left[f_c t + \frac{1}{2}\gamma_i h\left(\frac{t}{T_s} - i\right)\right] + \varphi_i\right\}, \quad iT_s \le t \le (i+1)T_s \tag{6a}$$

$$\varphi_i = h\pi\sum_{i=-\infty}^{i-1}\gamma_i \mod 2\pi \tag{6b}$$

- LRC (raised cosine):

$$g(t)=\begin{cases}\dfrac{1}{2LT_s}\left[1-\cos\left(\dfrac{2\pi t}{LT_s}\right)\right] & ,\ 0\le t\le LT_s\\ 0 & ,\ \text{elsewhere}\end{cases} \tag{7}$$

- GMSK (gaussian MSK):

$$g(t)=\frac{1}{2T_s}\left[Q\left(2\pi B_{3\text{dB}}\frac{t-T_s/2}{\sqrt{\ln 2}}\right)-Q\left(2\pi B_{3\text{dB}}\frac{t+T_s/2}{\sqrt{\ln 2}}\right)\right]$$
$$0\le B_{3\text{dB}}T_s<\infty \tag{8}$$

being $B_{3\text{dB}}$ the bandwidth at –3dB of the spectrum maximum.

CPFSK has paramount importance since it lower bounds what we can expect from a set of h and M, remembering that smother pulse shapes then 1REC will allow better spectrum efficiency, e.g. [1-2]. A larger M and shorter phase transitions (smaller h) produce the same effect. In CPFSK different frequencies can be detected during each interval T_s. Minimum shift keying (MSK) and Sünde's BFSK are particular cases with h=1/2 and h=1, respectively. Fig. 2 shows the three graphical presentations of CPM (for MSK).

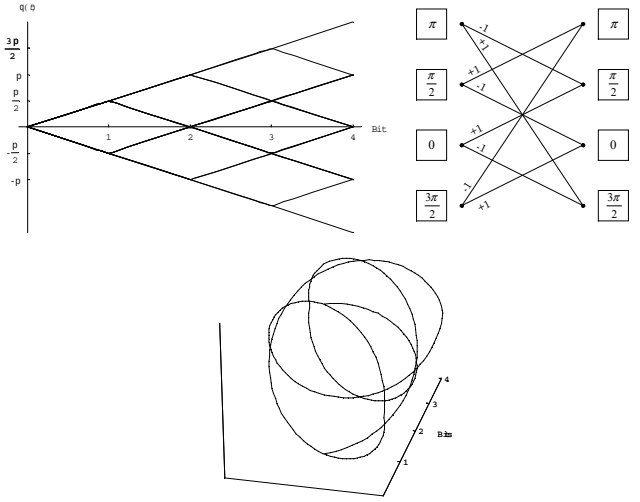

Fig. 2: MSK: phase tree; phase trellis and the phase cylinder (the later shows all possible complex phase progressions in time).

CPM states are defined as

$$S_i=\{\varphi_i,\gamma_{i-1},\gamma_{i-2},\ldots,\gamma_{i-L+1}\} \tag{9}$$

Hence the number of states related to the modulation is

$$S_M=q\cdot M^{L-1}\ ,\ \text{for even p} \tag{10a}$$

$$S_M=2q\cdot M^{L-1}\ ,\ \text{for odd p} \tag{10b}$$

This can be summarised by writing the modulation index as $h=2k/q$ (k and q integers). In this way $S_M=q\cdot M^{L-1}$, always.

B. Euclidean metrics and BER

In order to evaluate CPM performance one uses the *minimum euclidean distance* between two CPM signals transporting respectively the channel symbols sequences $\boldsymbol{\gamma}$ and $\boldsymbol{\gamma}'$:

$$D^2_{\min}(\boldsymbol{\gamma},\boldsymbol{\gamma}')=\int_0^{\infty}\left[s(t,\boldsymbol{\gamma})-s(t,\boldsymbol{\gamma}')\right]^2dt \tag{11}$$

It is useful to define the *minimum normalised squared euclidean distance* (MNSED) as

$$d^2_{\min}(\boldsymbol{\gamma},\boldsymbol{\gamma}')=\frac{D^2(\boldsymbol{\gamma},\boldsymbol{\gamma}')}{2E_s} \tag{12}$$

Using trigonometry, it can be showed [6-Sec.2.2.3] that

$$d^2_{\min}(\boldsymbol{\gamma},\boldsymbol{\gamma}')=\frac{\log M}{T_s}\int_{iT_s}^{(i+1)T_s}\left[1-\cos\left(\varphi(t,\boldsymbol{\gamma})-\varphi(t,\boldsymbol{\gamma}')\right)\right]^2dt \tag{13}$$

It can be interpreted as a cumulative sum of *incremental normalised euclidean distances* that occur during each one of the N_s symbols:

$$d^2_{\min}=2E_s\sum_{i=0}^{N_s-1}d_i^2 \tag{14}$$

Therefore, from (11), (12) and (14)

$$d_i^2=\frac{1}{2E_s}\int_{iT_s}^{(i+1)T_s}\left[s(t,\boldsymbol{\gamma})-s(t,\boldsymbol{\gamma}')\right]^2dt \tag{15}$$

Defining the phase differences between $\boldsymbol{\gamma}$ and $\boldsymbol{\gamma}'$ as

$$\Delta\varphi_i=\varphi(iT_s,\boldsymbol{\gamma})-\varphi(iT_s,\boldsymbol{\gamma}') \tag{16}$$

d_i^2 is also [6-pp.62]

$$d_i^2=\begin{cases}1-\dfrac{\operatorname{sen}\Delta\varphi_{i+1}-\operatorname{sen}\Delta\varphi_i}{\Delta\varphi_{i+1}-\Delta\varphi_i}, & \Delta\varphi_{i+1}\ne\Delta\varphi_i\\ 1-\cos\Delta\varphi_i, & \Delta\varphi_{i+1}=\Delta\varphi_i\end{cases} \tag{17}$$

(17) tells that d_i^2 is only dependent on what happens at the beginning and at the end of each T_s. It is also symmetrical in respect to a $\Delta\varphi_{i+1}$ and $\Delta\varphi_i$ exchange.

The bit error rate (BER) is, e.g. [6-pp.55]:

$$P_b\approx C\cdot Q\left(\sqrt{d^2_{\min}\frac{E_b}{N_0}}\right)\approx Q\left(\sqrt{d^2_{\min}\frac{E_b}{N_0}}\right) \tag{18}$$

C is a constant dependent on the signal space (≈1 in CPM). $Q(x)$ is the area under the unit variance gaussian probability distribution in $[x,\infty]$. Note that power efficiency comparisons can be made merely by $d^2_{\min}$ knowledge.

II. CODED CPM SCHEMES

The concatenation structure is depicted in Fig. 3.

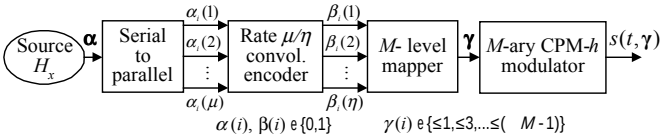

Fig. 3: Modulation and coding concatenation.

At every instant $t=iT_s$, the set of information bits coming from a discrete source with entropy Hx, $\{\alpha_i(1),\ \alpha_i(2),\ \cdots,\ \alpha_i(\mu)\}$, enter the coder which outputs the set $\{\beta_i(1),\ \beta_i(2),\cdots,\ \beta_i(\eta)\}$.

Table 1: Natural mapping in 8-CPM for a η=3 code.

$\{\beta_i\}$	000	001	010	011	100	101	110	111
γ_i	-7	-5	-3	-1	+1	+3	+5	+7

The coded channel symbols, γ_i, originate from a natural mapping of the coded stream $\boldsymbol{\beta}$ (see Table 1).

Complexity is measured in terms of the total number of states in the Markov chain to detect. There are $S=S_M \cdot S_C$ states, being $S_C=2^K$ associated to the encoder (of memory K), and S_M associated with the modulation, as settled in (10). Therefore:

$$S_M = q \cdot M^{L-1} \cdot 2^K \quad , \text{ for even } p \tag{19a}$$

$$S_M = 2q \cdot M^{L-1} \cdot 2^K \, , \text{ for odd } p \tag{19b}$$

The search for good concatenations of codes and M-ary signalling has been done exhaustively in the last decade. Applying set partition rules based on symmetries and Ungerboeck rules for trellis coded modulation (TCM), it has been proved by [7] that a search of codes observing those criteria conducts to the same coded CPM concatenations formerly encountered by heuristic procedures. There are 2 K=2, 10 K=3 and 44 K=4 codes observing those rules [7]. One of the best-known choices in terms of joint power and bandwidth performance makes use of rate $\upsilon=\mu/\eta=2/3$ encoders. Those perform much better than all $\upsilon=1/2$ codes. They all beat uncoded (3RC; M=4)-CPM.

Table 2: Best schemes in power-bandwidth terms. (Compiled from graphs in [2,7].)

υ	K	Code	$g(t)$	M	h	G_{MSK} [dB]	ζ_{99} [bps/Hz]	S
Uncoded			1REC	2	1/2	0	0.84	4
Uncoded			3RC	4	3/5	3.6	0.84	160
Uncoded			3RC	4	1/2	2.2	1.00	64
2/3	2	(7,2)	1REC	8	1/6	3.2	1.00	48
2/3	3	(15,2)	1REC	8	1/6	3.8	1.00	96
2/3	3	(15,2)	1REC	8	1/5	3.8	0.84	80
2/3	3	(15,2)	2RC	8	1/6	3.2	1.26	384
2/3	3	(13,4)	2RC	8	2/9	4.0	1.00	576
3/4	4	(33,4)[1]	1REC	16	2/15	4.5[2]	1.05	480
4/5	4	(33,4)[1]	1REC	32	2/15	5.7[2]	0.80	480

Table 2 presents nine schemes having good power and spectrum efficiency. MSK was added for easier evaluation. Remembering that MSK has a MNSED of 2, gains referenced to it are calculated by $G_{MSK}=10\log(d^2_{min}/2)$. ζ_{99} is the spectral efficiency linked to the 99% RF bandwidth. The number of states is obtained by (19).

CPFSK with ($\upsilon=2/3$; K=3; M=8; h=1/6) achieves the gain upper bound for 8-level CPM with $\upsilon=2/3$ encoders [2] with 96 states. It is certainly the best choice for a practical system.

In the following, the analysis is centred in the shadowed scheme of Table 2. It has an acceptable performance while having manageable complexity with its S=48 states. The elected code is defined by $g(x)$=[1 x^2+x+1 x+1] or (1,7,2) in octal (memory K=2), comprising $S_C=2^2$ states – see Fig. 4.

[1] From [6-Apendix D]

[2] Calculated from MNSED given in [6-Apendix D].

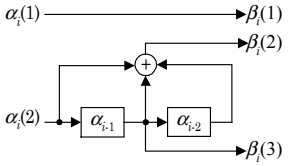

Fig. 4: Convolutional encoder (1,7,2), $\upsilon=2/3$, K=2.

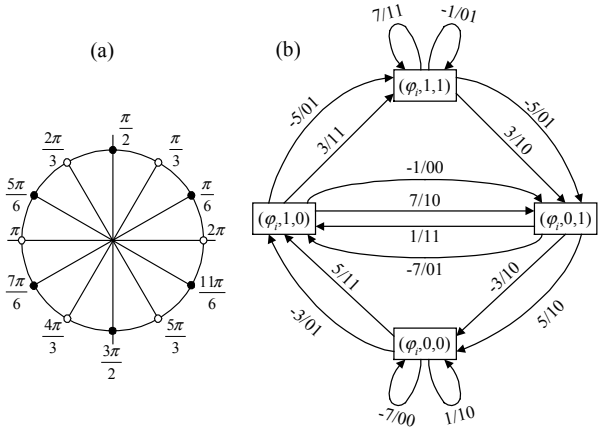

Fig. 5: States definitions. (a) Phase states for CPM h=1/6 (*odd* and *even states* are differentiated); (b) $\upsilon=2/3$, (1,7,2) encoding.

For every one of the possible 12 phase states at the beginning each interval, there are 2^K=4 possible states defined by the encoder (Fig. 5). One can now understand that the total Markov chain contains $S=2\times6\times2^2=48$ states.

It is preferable to introduce additional memory in the process by using external encoding rather by introducing partial response signalling. The later increases S by a factor M^{L-1}, where M is ≥2, while the former increases only by 2^K. Nevertheless, partial response signalling has the additional advantage of spectrum narrowing.

III. RADIO CHANNEL

In narrow-band wireless systems the signal is received after a noisy AWGN environment and a multiplicative distortion (flat Rayleigh fading). The latter is obtained by means of two independent gaussian processes (n_x and n_y). The received signal is

$$y(t,\boldsymbol{\beta}) = R(t) \cdot s(t,\boldsymbol{\beta}) + n(t) \tag{20a}$$

$$R(t) = \sqrt{n_x^2 + n_y^2} \tag{20b}$$

The physical continuity of a fading process always implies a filtering which is a function of the arriving rays model. The Aulins's model [8-Sec.5.4] is a good one, being more accurate one than classical Doppler filtering.

IV. RECEIVER COMPLEXITY REDUCTION

The introduction of channel coding added more complexity to the detection process. The optimum maximum likelihood sequence detection (MLSD), accomplished by a bench of 2M correlators (i.e., M for I and Q components) followed by a Viterbi detector, implies great complexity

especially when high M and/or weak modulation indices are used to enhance spectrum behaviour. The suitable Viterbi algorithm (VA) would then have an exponential growth on the number of paths to be stored. This complexity drawback increases if one remembers the issue of phase synchronization after a multipath-fading channel.

The first step in complexity reduction consists in taking into account that S can be cut in half. For the phase transitions γ_i defined (odd values) one sees that the states can be classified in two classes: *odd states* ($\{1\pi p/q,\ 3\pi p/q,\cdots,\ (2q\text{-}1)\pi p/q\}$) and *even states* ($\{0,\ 2\pi p/q,\ \cdots,\ (2q\text{-}2)\ \pi p/q\}$) – Fig 5(a). When a symbol interval ends, the possible states belong to just one of those two classes. So, at every iteration, the "effective" number of states for the (υ=2/3; K=2; M=8; h=1/6) scheme is S_{ef}=24.

A. Metric calculus in Walsh spaces

In the proposed receiver, the traditional bench of matched filters is replaced by a projection on an orthogonal signal space. The Walsh space [9-Sec3.3], chosen by [3], is used. This space is a trade-off between optimality and complexity. Fig. 6 shows the overall receiver structure.

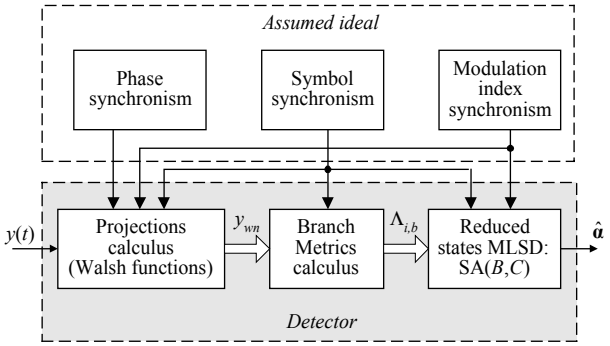

Fig. 6: Proposed detection for coded CPM: Walsh mapping and RRSD through the search algorithm.

The Walsh space supports an inner product and the spanning of $w_{F,n}(t)$ (Walsh functions) generates a completed space (all Cauchy signal sequences have their limit inside the space). Therefore it's a Hilbert space. Moreover, it has a normalised orthogonal base: the Walsh functions $w_{F,n}(t)$. F is the space dimension corresponding to the number of base functions, each one having F symbols. Walsh functions are denoted by

$$w_{F,n}(t) = \sum_{j=0}^{F-1} w_{F,n}[j] \cdot \mathrm{rect}\left[\frac{t - jT_s/2F}{T_s/2F}\right]$$

$$n=0,\ 1,\cdots,\ F\text{-}1=2^{u}\text{-}1\ (u\in\mathbb{Z}^{+}) \qquad (21)$$

where rect(t)=1 for 1/2<|t|<1/2 and zero elsewhere. $w_{F,n}[j] \in \{-1,\ +1\}$ and are specified by a recursive procedure that builds Walsh-Hadamard matrices [9].

Metrics calculations are made in the Walh space (as illustrated in Fig. 7), seeing that's reasonable to state:

$$y(t,\gamma_i) \approx y_w(t,\gamma_i) = \sum_{n=0}^{F-1} y_{wn} \cdot w_{F,n}(t - iT_s) \qquad (22)$$

Where $y_{wn} = \left\langle y(t,\gamma_i), w_{F,n}(t-iT_s)\right\rangle$, i.e,

$$y_{wn} = \int_{iT_s}^{(i+1)T_s} y(t,\gamma_i)\cdot w_{F,n}(t-iT_s)\,dt \qquad (23)$$

These coefficients are easily determined due to piecewise nature of Walsh functions:

$$y_{wn} = \sum_{j=0}^{F-1} w_{F,n}[j]\cdot \int_{(i+j/F)T_s}^{(i+(j+1)/F)T_s} y(t,\gamma_i)\,dt \qquad (24)$$

The description (21)-(24) also applies to all the possible transitions $s(t,\gamma_i)$ at $[iT_s,\ (i+1)T_s]$, defining the projection $s_w(t,\gamma_i) \approx s(t,\gamma_i)$. Note that its coefficients, s_{wn}, can be resolved in advance and can be memorized into the logic-processing unit represented in Fig 8(b). Fig. 7(a) depicts the w_8,$n(t)$ set. The integrator in (24) does not need to be dumped at every j sample. It can work continuously during T_s. From its output samples it is possible do know the partial integrations by subtracting the previous sample value.

The base functions must assume the form $A\cdot w_{F,n}(t)$. In order to $\|\psi_u\|^2=1,\ \forall u\in\mathbb{Z}^{+}$, i.e, $\int_0^{T_s} A^2\left[w_{F,n}(t)\right]^2 dt = 1$, it is immediate from (21) that A must be $\sqrt{1/T_s}$. Normalised base-band conversion also implies a $\sqrt{2/T_s}$ factor. So, one should have

$$\psi_1(t) = \sqrt{2}/T_s\ \cos\left(\omega_c t + \varphi(t,\gamma_i) + \varphi_i\right) \qquad (25a)$$

$$\psi_2(t) = \sqrt{2}/T_s\ \sin\left(\omega_c t + \varphi(t,\gamma_i) + \varphi_i\right) \qquad (25b)$$

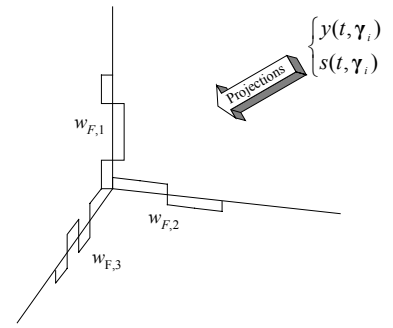

Fig. 7: Concept of projecting on a Walsh space the received signal and all possible transitions signals in $[iT_s,\ (i+1)T_s)]$. (Three dimensions of the F=4 case are depicted.)

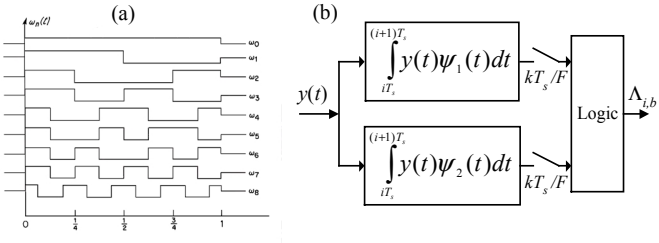

Fig. 8: Block for branch metrics calculus. (a) Walsh functions $w_{8,n}$; (b) hardware block.

The branch metrics are, for b=1, 2, ···, M:

$$\Lambda_{i,b} = d^2\left(y(t,\gamma_i), s(t,\gamma_b)\right) = \sum_{n=0}^{F-1} \left|y_{wn} - s_{wn}\right|^2 \qquad (26)$$

There are $S_{ef} \cdot M$ possible transitions. Applying (19), one gets $q \cdot M^L \cdot 2^K$ branches in the time variant trellis.

$\Lambda_{i,b}$ can be calculated by another way, due to:

$$d^2\left(y(t,\gamma_i), s(t,\gamma_b)\right) = \left\| y(t,\gamma_i), s(t,\gamma_b) \right\|^2 =$$

$$= \left\| y(t,\gamma_i) \right\|^2 + \left\| s(t,\gamma_b) \right\|^2 - 2\left\langle y(t,\gamma_i), s(t,\gamma_b) \right\rangle$$

$$= E_{yi} + E_{sb} - 2\left\langle y(t,\gamma_i), s(t,\gamma_b) \right\rangle \quad (27)$$

Notice that the energy of the received symbol, E_{yi}, is independent of the transition and, as well, the energies of the possible symbols are all the same (E_{sb}=E_s) – that's what permits (1). So, the metrics can be simply the inner product

$$\Lambda_{i,b} = \left\langle y(t,\gamma_i), s(t,\gamma_b) \right\rangle = \sum_{n=0}^{F-1} \left(y_{wn} \cdot s_{wn} \right)^2 \quad (28)$$

In this case, the MLSD must search the sequence having maximum metric and not the minimum.

Advantages of this receptor are: the receiver front-end is independent of the CPM scheme; reduced and common hardware is used; the number of states for MLSD is not increased. The downside is some degradation in $d^2_{\min}$, since it is evaluated with the projections. Being the space a completed one, $F \to \infty$ assures a performance closer to the one attained with metrics given by matched filters. F=4 has proved negligible performance degradation in AWGN [3]. Less significant losses are expected for smaller h, once that the signal's phase becomes more constant during intervals.

B. Sequences detection: the search algorithm

To accomplish RSSD the detector operates with the *search algorithm* [4,5]. This implements a separation of the S states into C classes, M_n (n=1,2,···,C). Hence, every class contains S/C states. Within each class some paths are discarded at each symbol decision. B is the number of paths chosen to remain in competition inside each class. This *search algorithm* and its variables are denoted by SA(B,C). One can recognize that the VA is a particular case of the SA, i.e., with a slight notation abuse, VA= SA(B=1,C=S). The entire SA(B,C) family performs MLSD [4]. The steps to be performed are [5]:

0: *Initiate path memory with a* start state. *There are now B·C paths in path memory.*

1: *Extend each old path into M new paths. Calculate the metric increment for each new branch and add the accumulated metrics of the old paths to obtain the new metrics. There are now M·B·C candidate paths.*

2: *Identify all mergers. Keep the one with the best metric and delete the others from the candidates.*

3: *Map each candidate path onto the corresponding state class. This will give C contender lists.*

4: *From each contender list select the B paths with best metric. Store the surviving paths and their metrics in path memory. If there are less than B paths in the contender list, assign metric ∞ to the remaining states - or zero if (28) is used.*

5: *Select the survivor with the best metric. Follow this path backward δ steps and output the encountered data symbol as a detected one. Go to* **1**.

V. CONCLUSIONS

The analysis is centred in a reduced complexity receiver for joint convolutional encoding and M-CPM. A choice of good schemes is made, considering bandwidth, power efficiency and complexity in terms of total number of states. The coded CPM has inherently an incorporable number of states for a Viterbi Algorithm preceded by a typical bench of matched filters (or equivalent correlators). This complexity drawback is mitigated by simultaneous demodulation and decoding implementing complexity reduction concepts. Simplifications at both two receivers stages were introduced, hence, the receiver is sub-optimum. Metrics are computed on a F dimensions Walsh space. Projecting the received signal into it only requires two integrators and a sampling procedure. A single reduced states sequence detector (RSSD) using the search algorithm performs a significant memory reduction by eliminating some possible branch propagations. The proposed receiver accomplishes a near-optimum performance while having a complexity feasible in actual digital signal processing (DSP) hardware. Multi-h systems can also be considered. A time variant trellis exists even in single-h CPM. So, only variant transitions must be added.

REFERENCES

[1] T. Aulin and C. Sundberg, "Continuous Phase Modulation - Part I: Full Response Signalling", *IEEE Trans. on Comm.*, vol. Com-29, no. 3, pp. 196-209, Mar. 1981.

[2] J. B. Anderson and C. Sundberg, "Advances in Constant Envelop Coded Modulation", *IEEE Comm. Mag.*, vol. 29, no. 12, pp. 36-45, Dec. 1991.

[3] T. Svensson, A. Svensson, "Reduced Complexity Detection of Bandwidth Efficient Partial Response CPM," *in Proc. of IEEE VTC'99*, Houston, Texas, pp. 1296-1300, May 1999.

[4] T. Aulin, "Breadth-First Maximum Likelihood Sequence Detection", *IEEE Trans. on Comm.*, vol. 47, no. 2, pp. 208-216, Feb. 1999.

[5] A. Cedergren, *Maximum likelihood Sequence Detection by Using the SA(B,C) Algorithm – State Partition Methods*, Licenciate Thesis, Dep. of Comp. Eng., Chalmers Univ. of Technology, Sweden, 2000.

[6] J. Anderson, T. Aulin, C. Sundberg, Digital Phase Modulation, Plennum Press, New York, 1986.

[7] P. Ho and P. McLane, "Spectrum, Distance, and Receiver Complexity of Encoded Continuous Phase Modulation", *IEEE Trans. on Inf. Theory*, vol. 34, no 5, pp. 1021-1032, Sep. 1988.

[8] J. Parsons, *The mobile Radio Propagation Channel*, Pentech Press, London, 1992.

[9] L. E. Franks, *Signal Theory*, Prentice-Hall, 1969.